Progress In Electromagnetics Research, PIER 99, 323–338, 2009

ANALYTICAL AND NUMERICAL ANALYSES OF A CURRENT SENSOR USING NON LINEAR EFFECTS IN A FLEXIBLE MAGNETIC TRANSDUCER

E. Vourc'h and P.-Y. Joubert

SATIE, ENS Cachan, PRES UniverSud
61 Avenue du Président Wilson, Cachan 94230, France

L. Cima

Billanco SA
194 Avenue Aristide Briand, Cachan 94230, France

Abstract—A theoretical study and a simulation method are proposed for superparamagnetic current sensors implementing a uniformly wound toroidal core topology. So as to be easy to implement, this sensor topology can be made flexible thanks to the use of a core made up of a superparamagnetic powder embedded in a flexible plastic matrix. The measurement of DC and AC currents is possible provided that a sinusoidal magnetic field excitation is applied to the superparamagnetic transducer. An analytical model is proposed for computing the sensor output signal and we demonstrate that when the detection of the component at the second order harmonic of the excitation frequency is used, the measurement is independent of the conductor position in a given current range. For simulating the dynamic response of the sensor, we propose to combine the analytical model, or a finite elements model, with a time-discretization method. Furthermore, simulations are carried out considering a ring shaped sensor and the real magnetization characteristics of a superparamagnetic material. Simulations are provided over the [−10 kA 10 kA] range and for various amplitudes of the excitation signal. The results obtained with the analytical model, which is computationally efficient, are within 4% to 12.7% from the numerical results.

Corresponding author: E. Vourc'h (vourch@satie.ens-cachan.fr).

1. INTRODUCTION

There is a variety of current sensors dedicated to power electronics applications [1, 2]. This variety originates from the multiplicity of industrial requirements: either measurement performances or size or practical implementation constraints. To quote only two examples: the fluxgate sensors [3] enable the measurement of AC and DC currents and are reputed having a high accuracy especially when implemented in a closed loop configuration, while the Rogowski coils [4], which are AC only current sensors, exhibit a high dynamic range (up to a few tens of thousands of Amperes) and, with appropriate design, immunity to some external magnetic disturbances. Moreover, thanks to a flexible structure, they may also provide implementation facilities.

The concept of a new sensor implementing a superparamagnetic (SPM) core and dedicated to the measurement of large range AC/DC currents has recently been proposed and experimentally demonstrated [5, 6]. In this paper, the authors propose the theoretical study of an SPM sensor topology combining some advantages of fluxgate sensors (accurate AC/DC current measurement) and Rogowski coils (large dynamic range, flexible structure and immunity to disturbances).

Likewise fluxgates, SPM sensors take advantage of the non-linearity of their core magnetization characteristic. They are subjected to two stresses: first the magnetic field due to the current to measure, which fixes a bias point on the core magnetization curve; and second, a variable magnetic field produced by an excitation winding. The measurement of the current may be performed via lock-in amplification at the second order harmonic of the excitation frequency of the electromotive force (EMF) at the ends of a sensing coil. With regards to the sensor topology, with a view to achieve independency of the measurement with respect to the position of the sensor, following the example of Rogowski coils, it seems judicious to choose a uniformly wound SPM torus surrounding the conductor fed by the measured current. Moreover, the SPM material may be embedded in a flexible plastic matrix (at the image of the SPMFlex sensors developed by the Billanco company) so that the sensor is easy to implement likewise Rogowski coils too.

The prospects of SPM materials for the measurement of high currents and some interests of the toroidal topology are discussed in Section 2. In Section 3, a theoretical study is proposed to assess the output signal of such sensors. We demonstrate that when an appropriate detection method is used, within a wide current range, the measurement can be made independent of the position of the conductor

surrounded by the core. In Section 4, we develop an analytical model for the considered sensor, which enables computationally efficient simulations to be carried out [7]. This model is implemented using a time-discretization method so as to determine the non linear dynamic response of the sensor. Besides, numerical simulations based on finite elements modelling allow the accurate geometry and features of the studied electromagnetic problem to be taken into account [8–10]. Therefore, with a view to validate the proposed analytical model, analytical and numerical simulations of a toroidal SPM sensor, considering the real characteristics of an SPM material, are carried out and compared. Finally, conclusions are provided in section 5.

2. FLEXIBLE, CLOSED AND UNIFORMLY WOUND SPM TRANSDUCER TOPOLOGY FOR CURRENT MEASUREMENT

An SPM material results from the reduction of a ferromagnetic material into a nanoparticular powder. The thus obtained nanoparticles consist in single Weiss domains and it is the disappearance of the Bloch walls that eliminates the hysteresis phenomenon in the macroscopic magnetization curve of the material. Indeed the magnetization of the material has no longer a ferromagnetic behaviour but is similar to paramagnetism with a higher susceptibility. This behaviour discovered by Néel [11, 12] was later called the superparamagnetism [13, 14].

To date, most applications of SPM materials fall into the biomedical field [15–17]. Polymer or inorganic microbeads embedding SPM nanoparticles are used for cell separation or as contrast agents in magnetic resonance imaging. In those cases, it is the ability of SPM particles to be selected by means of an applied magnetic field that is exploited. There also exist ferrofluids consisting in suspensions of SPM particles inside a fluid. They may be used in machine clutches or magnetic seals in motors [18, 19].

Besides, thanks to their non linear and hysteresis free magnetization behaviour, SPM materials may also be useful to measure currents. For such an application raw SPM powders seem inappropriate, however, it is possible to load SPM nanoparticles inside a bulk plastic matrix. Thus, solid, easy to shape and even flexible SPM cores can be envisaged.

Basically, an SPM current sensor is a magnetic field sensor. It consists in a SPM core featuring a driving coil and a sensing coil both wound around the core. The driving coil is fed by a high frequency AC current so as to generate an EMF at the ends of the sensing coil,

whether the measured current is AC or DC. The current to be measured induces a bias magnetic field within the SPM core while the excitation current imposes a variation around the bias point. Obviously, the sensor output EMF will be dependent on the bias point corresponding to the measured current and the fact that the whole magnetization characteristic of an SPM material is non-linear, enables envisaging the measurement of currents over a large range.

Besides, experimental demonstration of the concept of SPM current sensors has been reported in [6]. The measurements were carried out over the −500 A to 500 A current range. In the proof of concept device, the transducer that was used did consist in a pair of parallelepiped bulk plastic matrices loaded with SPM particles.

Here, we propose a different kind of a topology inspired from Rogowski coils (Figure 1): a flexible plastic torus loaded with SPM particles, surrounding the conductor in which the current to measure flows. The sensing and the driving coils are assumed to be uniformly wound all around the core. The measured EMF can be decomposed into several contributions. First, the contribution of interest which is due to the T_1 turns that are parallel to the core

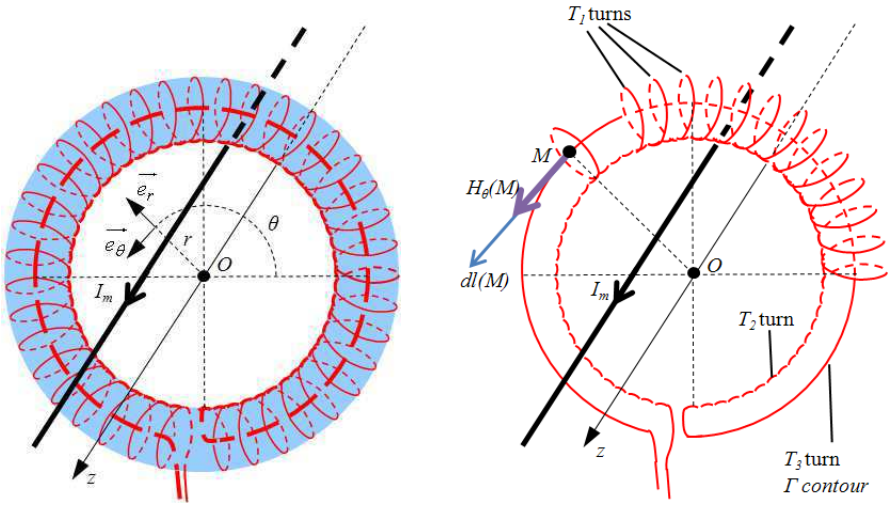

Figure 1. (a) SPM current sensor implementing a uniformly wound topology (for clarity of the drawing the excitation winding is not represented). (b) Display of the three types of turns constituting the sensing coil.

cross section (Figure 1(b)). Second, a T_2 turn (Figure 1(b)) equivalent to the wires that connect the T_1 turns to each other and that may deliver an unwanted EMF due to possible perturbation magnetic field components along the z axis of the core. However, it is to be noted that unlike Rogowski coils, here, only an AC perturbation at the first or the second order harmonics of the excitation frequency could be deleterious. Should such a high frequency perturbation occur, its effect could be easily overcome thanks to a judicious choice of the excitation frequency. Hence, the implementation of an additional T_3 return turn (Figure 1(b)), wound in phase-opposition to T_2 so as to compensate for the contribution of T_2, is not mandatory. In summary, it is the non-linearity of SPM materials magnetization curves that makes them suitable for the measurement of high currents. Using a sinusoidal excitation (and detection at the second order harmonic of the excitation frequency) it is possible to measure AC as well as DC currents, provided that the excitation frequency is significantly higher than that of the measured current. Moreover, provided the use of an SPM material such that its magnetic particles are smaller than a critical size, and choosing an excitation frequency lower than a critical limit, the material is hysteresis free [20, 21] and allows for AC and DC accurate operations of the sensor to be carried out. With regards to the sensor topology, a flexible toroidal structure, (made possible by plastic matrices embedding SPM nanoparticles) surrounding the conductor and uniformly wound offers several advantages: in situ implementation facility, and also a measurement independent of the position of the conductor, as shown in the following theoretical study.

3. THEORETICAL STUDY

The SPM current sensor topology to be modelled consists in a closed core with toroidal shape featuring sensing and driving coils, both uniformly wound along the torus.

The sensor behaviour is intrinsically linked to the magnetization characteristics of the SPM material. For the sake of the reasoning our study will refer to the characteristics of a maghemite SPM sample measured by means of a vibrating sample magnetometer (Figure 2).

Firstly, we will give an analytical expression for the EMF delivered by one sensing winding. Secondly, in the light of this expression, we will consider the opportuneness of detecting the EMF harmonic at the second order of the excitation frequency for determining the value of the measured current. Next, assuming such a detection, we will give an expression for the sensor output signal and analyse it with regards to the influence of the position of the primary conductor with respect

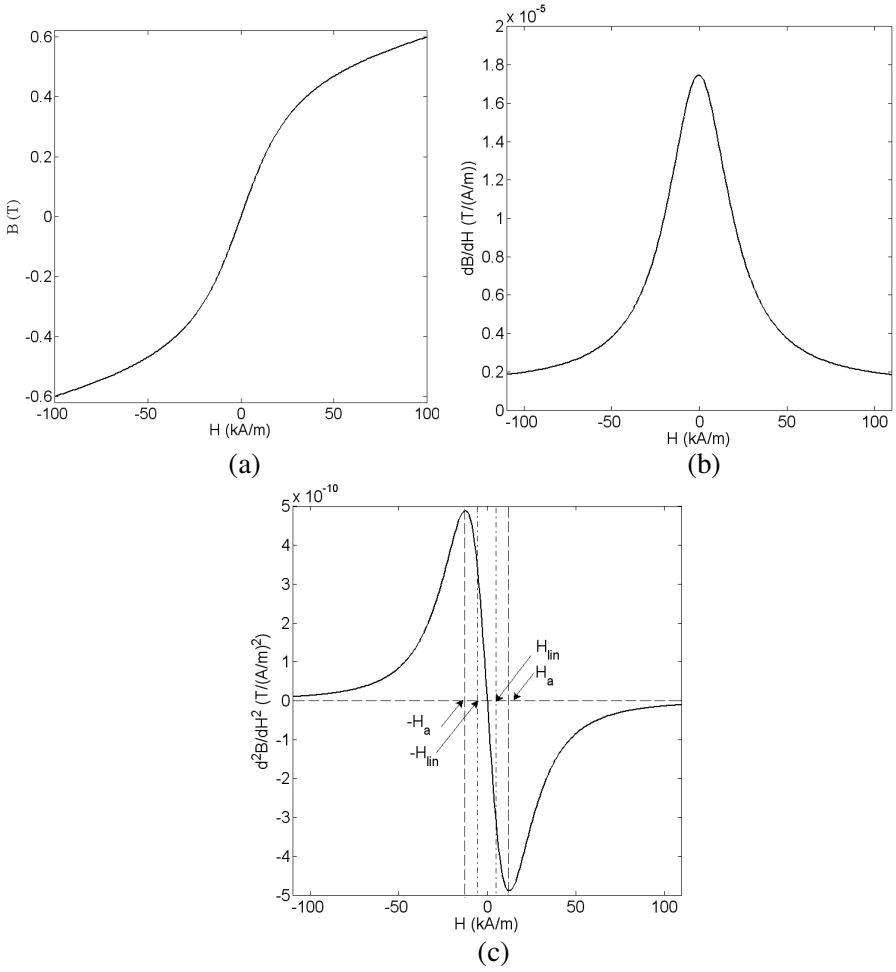

Figure 2. Characteristics of the considered SPM material (maghemite nanoparticles embedded in a plastic matrix) derived from LakeShore 7310 VSM measurements. (a) B(H) magnetization curve, (b) first derivative of the B(H) magnetization curve, (c) second derivative of the B(H) magnetization curve.

to the transducer.

3.1. Analytical Model for the SPM Sensor Output EMF

Let us consider an SPM torus of revolution axis z, of cross-sectional area S and of average radius R. Let n_{ex} and n_{sens} be the number

of excitation and sensing turns per meter along the Γ average circumference of the torus respectively. The conductor fed by the I_m current to measure, which is surrounded by the torus, is assumed to be parallel to z but not necessarily placed at the centre of the torus.

The sensing coil is sensitive to the azimuthal component of the magnetic field intensity, H_θ. According to the superposition principle, H_θ is the sum of the field $H_{m\theta}$ due to I_m and of the time varying $H_{ex\theta}(t)$ excitation magnetic field induced by the sinusoidal current $i_{ex}(t) = I_{ex}\sin(\omega_{ex}t)$ feeding the driving coil.

Assuming that H_θ is homogeneous on the torus cross section, it is possible to give an analytical expression for the $\varepsilon(t)$ EMF at the ends of a sensing turn.

For the sake of simplicity, in the following, $H_\theta(t, M)$, $H_{m\theta}(M)$, $H_{ex\theta}(t, M)$ will be denoted H, H_m and H_{ex} respectively. In the same manner, the magnetic field density $B_\theta(t, M)$ will be denoted B.

The second-order Taylor's expansion of B centred at H_m is

$$B(H) = B(H_m) + (H - H_m)\left.\frac{\partial B}{\partial H}\right|_{H_m} + \frac{(H - H_m)^2}{2}\left.\frac{\partial^2 B}{\partial H^2}\right|_{H_m} \quad (1)$$

By introducing the small signal magnetic permeability $\mu_r = \frac{1}{\mu_0}\frac{\partial B}{\partial H}$, where μ_0 is the permeability of vacuum, (1) may be rewritten as

$$B(H) = B(H_m) + (H - H_m)\,\mu_0\mu_r(H_m) + \mu_0\frac{(H - H_m)^2}{2}\left.\frac{\partial \mu_r}{\partial H}\right|_{H_m} \quad (2)$$

It follows that the EMF $\varepsilon(t)$ delivered by one sensing turn is given by

$$\begin{aligned}\varepsilon(t) &= -S\frac{\partial}{\partial t}B(H_m) - S\mu_0\mu_r(H_m)\frac{\partial}{\partial t}(H - H_m)\\ &\quad -S\mu_0\left.\frac{\partial \mu_r}{\partial H}\right|_{H_m}\frac{\partial}{\partial t}\left[\frac{(H - H_m)^2}{2}\right]\\ &= -S\mu_0\mu_r(H_m)\frac{\partial}{\partial t}(H) - S\mu_0\left.\frac{\partial \mu_r}{\partial H}\right|_{H_m}\cdot(H - H_m)\frac{\partial H}{\partial t} \quad (3)\end{aligned}$$

Since $H(t) = H_m + H_{ex}(t)$ and with the hypothesis of a sinusoidal magnetic excitation $H_{ex}(t) = h_{ex}\sin(\omega_{ex}t)$, $\varepsilon(t)$ becomes

$$\varepsilon(t) = -S\mu_0\mu_r(H_m)\,h_{ex}\cos(\omega_{ex}t) - S\mu_0\left.\frac{\partial \mu_r}{\partial H}\right|_{H_m}\frac{\omega_{ex}}{2}h_{ex}^2\sin(2\omega_{ex}t) \quad (4)$$

Thus, the sensed EMF contains a term at ω_{ex} and a term at $2\omega_{ex}$. Their amplitudes are proportional to $\left.\frac{\partial B}{\partial H}\right|_{H_m} = \mu_0\mu_r(H_m)$ and to $\left.\frac{\partial^2 B}{\partial H^2}\right|_{H_m} = \mu_0\left.\frac{\partial \mu_r}{\partial H}\right|_{H_m}$, which are the first and the second derivatives

of the magnetisation curve of the SPM material with respect to H, respectively.

Since $\frac{\partial B}{\partial H}$ is an even function (Figure 2(b)), the determination of H_m from the measurement of the component of $\varepsilon(t)$ at ω_{ex} would lead to an ambiguity on the sign of H_m.

Because $\frac{\partial^2 B}{\partial H^2}$ is an odd function which is monotonous in a range $[-H_a,\ H_a]$ (Figure 2(c)), to avoid ambiguity on the sign of H_m and subsequently on that of I_m, it is preferable to detect the component of $\varepsilon(t)$ at $2\omega_{ex}$.

Moreover, according to (Figure 2(c)), it is worth noting that conversely to the term at ω_{ex}, the term of $\varepsilon(t)$ at $2\omega_{ex}$ is null for $H = 0$. From the practical point of view, the detection of the e_2 amplitude of the component of the sensor output signal at the second order harmonic of the excitation frequency could be performed by means of a lock-in amplifier.

Let $de_2(M)$ be the contribution to e_2 of the $n_{sens} \cdot dl(M)$ sensing turns contained in the *dl(M)* long torus portion centred on M.

$$de_2\,(M) = -n_{sens} dl(M) S\mu_0 \left.\frac{\partial \mu_r}{\partial H}\right|_{H_m(M)} \frac{\omega_{ex}}{2} h_{ex}^2\,(M) \tag{5}$$

Subsequently

$$e_2 = \oint_\Gamma de_2\,(M) = -n_{sens} S\mu_0 \frac{\omega_{ex}}{2} \oint_\Gamma \left.\frac{\partial \mu_r}{\partial H}\right|_{H_{m(M)}} h_{ex}^2\,(M)\, dl\,(M) \tag{6}$$

As for symmetry reasons $h_{ex}(M)$ is independent of M it follows

$$e_2 = -n_{sens} S\mu_0 \frac{\omega_{ex}}{2} h_{ex}^2 \oint_\Gamma \left.\frac{\partial \mu_r}{\partial H}\right|_{H_{m(M)}} dl\,(M) \tag{7}$$

3.2. Study of the Dependency of the Measurement on the Cable Position

In the above expression of the sensor output signal, no hypothesis is made regarding the position of the conductor fed by I_m within the contour Γ.

In case the conductor is positioned at the centre of Γ, for symmetry reasons, $H_m\,(M)$ is independant of M and (2) simplifies as

$$e_2 = -n_{sens} S\mu_0 \pi R\omega_{ex} h_{ex}^2 \left.\frac{\partial \mu_r}{\partial H}\right|_{H_m} \tag{8}$$

However, if the I_m current to measure belongs to the $[-I_{lin}\ I_{lin}]$ range such that the induced H_m field is within the $[-H_{lin}\ H_{lin}]$ range where

$\mu_0 \frac{\partial \mu_r}{\partial H}$ is linear (Figure 2(c)), then

$$e_2 = -n_{sens} S \frac{\omega_{ex}}{2} h_{ex}^2 A \oint_{\Gamma} H_m(M) dl(M) \tag{9}$$

where A denotes the slope of the linear zone of $\mu_0 \frac{\partial \mu_r}{\partial H}$.

Moreover, according to Ampere's law, $\oint_{\Gamma} H_m(M) dl(M) = I_m$, which implies that the result of (9) is independent of the position of the conductor within Γ. Then,

$$e_2 = -n_{sens} S \frac{\omega_{ex}}{2} h_{ex}^2 A I_m \tag{10}$$

Still according to Ampere's law, it can be shown that $h_{ex} = n_{ex} I_{ex}$, which finally leads to

$$e_2 = -n_{sens} n_{ex}^2 I_{ex}^2 S \frac{\omega_{ex}}{2} A I_m \tag{11}$$

Typically, the linear range of the second derivative of the magnetization curve of an SPM material is in the order of a few kA·m^{-1}. Such feature should confer SPM current sensors with a measurement range independent of the conductor position in the order of a few hundreds or thousands of amperes, depending on the diameter of the SPM core. Nevertheless, the higher the core diameter, the lower the sensitivity of the sensor.

It is also to be noted that the EMF sensed by a Rogowski coil is independent of the position of the conductor and also of the shape of the amagnetic wound core. With regards to the particular SPM sensor topology considered in this article, it is not the total sensed EMF that may be independent of the position of the conductor, but only its component at $2\omega_{ex}$. Moreover, such independency requires the core contour Γ to be a circle.

Nevertheless, thanks to its excitation system, an SPM toroidal sensor enables measuring AC and DC currents while Rogowski coils only measure AC currents.

4. ANALYTICAL AND NUMERICAL SIMULATIONS

It is possible to give an analytical expression for the magnetic flux sensed by a uniformly wound ring SPM current sensor. In this section, we propose to combine such an analytical model, or a finite elements model, with a time discretization method in order to simulate the dynamic response of the sensor.

4.1. Sensor Dynamic Response Simulation Method

Assuming that the conductor fed by the I_m current to measure is centred with respect to the ring; for symmetry reasons, the magnetic fluxes sensed by every sensing turns are equal. Therefore, assuming the magnetic field intensity is homogenous on a cross section of the transducer, the whole flux sensed at the instant t is given by

$$\Phi(t) = 2\pi R n_{mes} S \cdot B(H(t)) \tag{12}$$

where the instantaneous magnetic field intensity $H(t)$ can be decomposed as $H(t) = H_m + H_{ex}(t)$.

Moreover, according to Ampere's law

$$H_m = \frac{I_m}{2\pi R} \text{ and } H_{ex}(t) = n_{ex} i_{ex}(t) = n_{ex} I_{ex} \sin(\omega_{ex} t) \tag{13}$$

Hence

$$\Phi(t) = 2\pi R n_{mes} S \cdot B\left(\frac{I_m}{2\pi R} + n_{ex} I_{ex} \sin(\omega_{ex} t)\right) \tag{14}$$

Thus, provided the magnetization curve $B(H)$ of the core material (Figure 2(a)), (14) enables computing the magnetic flux sensed at any instant t. For determining h_1 and h_2, the amplitudes of the components of the sensor output EMF at the first and second order harmonics of the excitation frequency, we propose the following method: first, $\Phi(t)$ is discretized on an excitation period with N samples. Second, the a_n and b_n $(n = 1, 2)$ coefficients of the Fourier series expansion of $\Phi(t)$ are derived from the samples as follows

$$a_n = \frac{2}{N} \sum_{k=0}^{N-1} \Phi(kT_0) \cos\left(n \frac{2\pi k}{N}\right) \tag{15}$$

$$b_n = \frac{2}{N} \sum_{k=0}^{N-1} \Phi(kT_0) \sin\left(n \frac{2\pi k}{N}\right) \tag{16}$$

where $T_0 = 2\pi / N\omega_{ex}$ is the sampling period. Third, the EMF being the time derivative of $\Phi(t)$, h_1 and h_2 are finally deduced from a_n and b_n according to (17).

$$|h_n| = n 2\pi f_{ex} \sqrt{a_n^2 + b_n^2} \tag{17}$$

In order to evaluate the above analytical model, simulations are performed and compared to data from numerical modelling.

Let us consider a sensor with a ring core of average radius $R = 27.5\,\text{mm}$ and of cross section radius $R_1 = 5\,\text{mm}$. The number of excitation and sensing turns are chosen to be $N_{ex} = 200$ and

$N_{sens} = 1000$ respectively, which corresponds to $n_{ex} = 1157.5$ and $n_{mes} = 5787.5$ turns per meter. The frequency of the excitation current is chosen to be $f_{ex} = 50\,\text{kHz}$ and the three following values $I_{ex} = 150\,\text{mA}$, $I_{ex} = 300\,\text{mA}$ and $I_{ex} = 500\,\text{mA}$ are considered for its intensity. Furthermore, the magnetization characteristic of the core material is considered to be the curve depicted in Figure 2(a) which results from the experimental characterization of a plastic sample loaded with maghemite SPM particles such that the load of particles represents 80% of the sample volume. The characterization was carried out using a LakeShore 7310 vibrating sample magnetometer (VSM).

The h_1 and h_2 components of the sensor output EMF are simulated by implementing the analytical model (14) and the sampling method described above and by iterating these computations for values of I_m ranging from $-10\,\text{kA}$ to $10\,\text{kA}$.

On the other hand, numerical simulations are carried out. This time, the magnetic flux captured by the considered sensor is computed thanks to 3D finite elements modelling using an edge flux based formulation of the considered magneto-dynamic problem and taking the non linear characteristic of the transducer into account. Besides, for simulating the dynamic response of the sensor and determining h_1 and h_2, the same discretization method as for the analytical model is used. Again, these simulations are iterated for values of I_m ranging from $-10\,\text{kA}$ to $10\,\text{kA}$.

4.2. Simulation Results Analysis

Results from both analytical and numerical simulations are shown in Figure 3. First, a qualitative result may be noticed: the variations of h_1 and h_2 as a function of the measured current are similar to those of the first and the second derivatives of the SPM material magnetization curve with respect to the magnetic field intensity respectively (Figures 2(b), (c)). This is consistent with the theoretical study of Section 3. Second, the analytical model results are in good agreement with the numerical data. With regards to h_1, the maximum distance between analytical simulations and numerical simulations for $I_{ex} = 150\,\text{mA}$, $I_{ex} = 300\,\text{mA}$ and $I_{ex} = 500\,\text{mA}$ are in the order of 1%, 1.2% and 5.3% respectively. With regards to h_2, these distances are 12.7%, 11% and 4.1% respectively. Such differences may be imputable to the analytical model simplifications, the main of which being the assumption of a homogeneous magnetic field intensity on the core section, as well as to the computation noise inherent in the finite elements modelling. Nevertheless, the good agreement between these simulations validates the accuracy of the proposed analytical model.

Furthermore, it is to be noted that the amplitude of the h_1

component of the sensed EMF is as high as a few tens or even hundreds of volts, depending on I_{ex} (Figure 3(a)). As pointed out in Section 3, contrary to h_2, the measurement of h_1 does not allow for determining the sign of the measured current. From the practical point of view

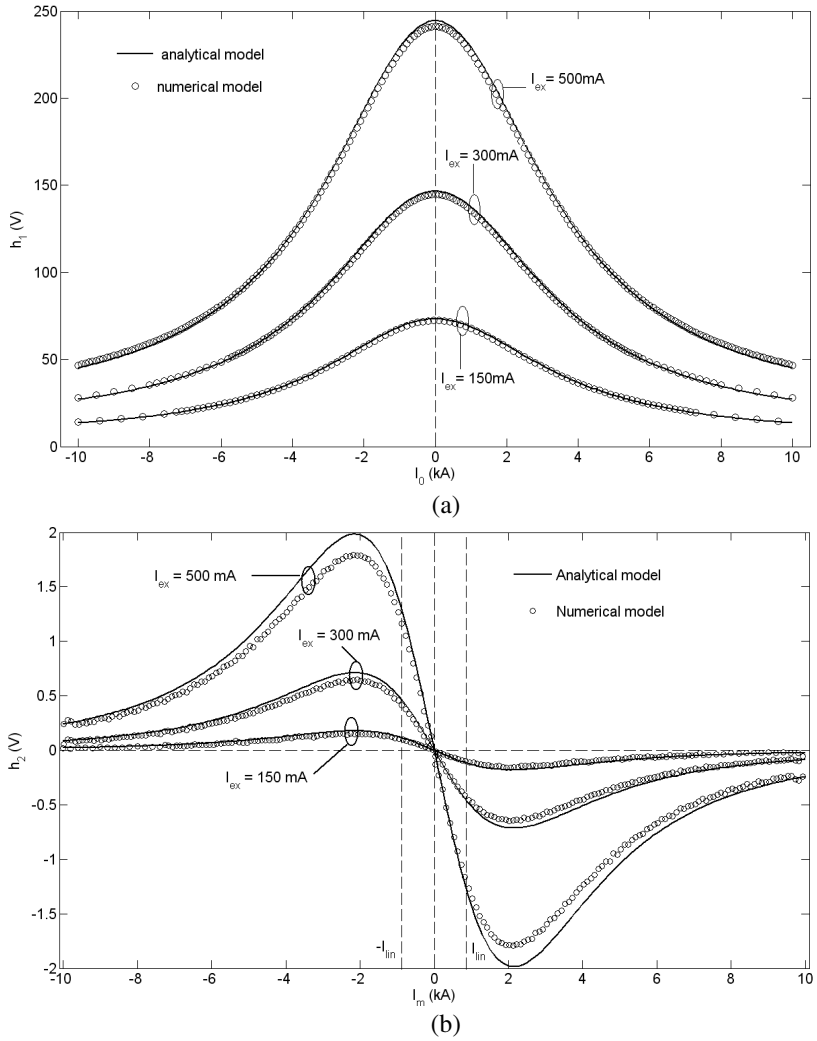

Figure 3. (a) Simulation results for h_1, the first order harmonic component of the EMF at the output of the toroidal SPM sensor. (b) Simulation results for h_2, the second order harmonic component of the EMF at the output of the toroidal SPM sensor.

the measurement of h_2 relies on the lock-in amplification of the sensed EMF at $2\omega_{ex}$. In order not to saturate the amplifier the h_1 component should be cancelled. To this aim, a differential sensor using two wound SPM cores could be used like what was done experimentally in [5], which incidentally would also double the level of h_2.

Although the assumption of small excitation amplitude made for the model developed in Section 3 is not strictly fulfilled, simulations show that the amplitude of h_2 varies proportionally to the square of the excitation current I_{ex} which also agrees with (11). According to Figure 3(b), the linear measurement range of the simulated sensor is up to about $I_{lin} = 700\,\mathrm{A}$. Such a feature is intrinsically linked to the characteristics of the SPM material that is considered. Indeed, according to the VSM characterization of the few maghemite SPM samples at our disposal, the extent of the linear range of $\frac{\partial^2 B}{\partial H^2}$, the second derivative of the measured magnetization curves appeared to be dependent on the size of the nanoparticles, which was the parameter that varied from a sample to another.

Note that, still according to the theoretical study of Section 3, for values of the measured current contained in $[-I_{lin}\ I_{lin}]$, the measurement should be independent of the conductor position with respect to the SPM transducer.

With regards to the sensor sensitivity, which is defined as the slope of the linear part of curve h_2, it is $-0.14\,\mathrm{mV/A}$, $-0.55\,\mathrm{mV/A}$ and $-1.6\,\mathrm{mV/A}$ for $I_{ex} = 150\,\mathrm{mA}$, $I_{ex} = 300\,\mathrm{mA}$ and $I_{ex} = 500\,\mathrm{mA}$ respectively. Comparison with the corresponding results given by the numerical model, shows that the sensitivity resulting from the analytical model is higher, with a relative difference that does not exceed 14% as far as the three considered cases are concerned.

Furthermore, the dynamic range of the sensor, which is the current range for which the curve h_2 is monotonous, is $2\,\mathrm{kA}$ wide, either according to the analytical or to the numerical model. Likewise the linear operating range, this feature is intrinsically linked to the characteristics of the SPM material that is considered.

However, the parameters of the sensor that was simulated (the dimensions, the number of winding turns, the excitation frequency, the excitation current intensity, the material characteristics) were chosen to be realistic, it should be pointed out that the simulations reported here do not pretend to assess the performances of an optimized ring SPM sensor. Our main purpose was to give an analytical model for the proposed sensor topology that could be used as a design tool that would be computationally efficient if compared with the use of a numerical software. Our purpose was also to investigate the accuracy of this analytical model by comparing its results to numerical simulations.

5. CONCLUSION

SPM current sensors have been proposed very recently for measuring AC and DC currents over ranges in the order of a few hundreds or thousands of amperes and experimental demonstration was carried out. Here we have theoretically investigated the prospects of a particular SPM current sensor topology consisting in a ring transducer uniformly wound with both an excitation and a sensing winding. The fact that the sensor surrounds the conductor fed by the measured current, enables minimizing for external magnetic disturbances. Moreover, the use of a flexible core consisting in a plastic matrix embedding SPM particles may facilitate the in situ implementation. An analytical study has been developed for this sensor topology. It has appeared that the detection of the component of the output EMF at the second order harmonic of the excitation frequency is suitable for being able to determine the current without a sign ambiguity. In addition, it was also demonstrated that within a given current range, the measurement should be insensitive to the position of the core with respect to that of the surrounded conductor. Furthermore, a method for modelling the dynamic response of the sensor has been proposed which combines an analytical expression for the instantaneous sensed magnetic flux with a time-discretization of this flux on a period of the driving signal. Simulations have been carried out considering a sensor example for which the SPM core magnetization curve did result from the characterization of an actual plastic sample loaded with maghemite SPM particles.

Qualitatively, the results of the simulations based on the analytical model are consistent with the theoretical study and quantitatively the good agreement with results from 3D finite elements modelling has shown the accuracy of the analytical model.

Further works will be dedicated to the experimental set up and characterization of a flexible toroidal SPM sensor. An emphasis will be placed on the design of the windings and of the instrumentation circuits used to reach accurate measurement of the output signal at the first and second order harmonics of the excitation frequency.

ACKNOWLEDGMENT

The authors thank Pr. Frederic Mazaleyrat for the SPM material characterization and for useful discussions on magnetic materials.

REFERENCES

1. Costa, F., P. Poulichet, F. Mazaleyrat, and E. Labouré, "The current sensors in power electronics, a review," *EPE Journal*, Vol. 11, No. 1, 7–18, 2001.
2. Ripka, P., "Sensors based on bulk soft magnetic materials: Advances and challenges," *J. Magn. Magn. Mater.*, Vol. 320, 2466–2473, 2008.
3. Ripka, P., "Advances in fluxgate sensors," *Sens. Actuators A*, Vol. 106, 8–14, 2003.
4. Ray, W., "Wide bandwidth Rogowski current transducers, Part 1: The Rogowski coil," *EPE Journal*, Vol. 3, No. 1, 51–59, 1993.
5. Lenglet, L., "Current & magnetic field sensors, control method & magnetic core for said sensors," *Billanco Patent WO2007042646 (A1)*, 2007.
6. Vourc'h, E., P. Y. Joubert, G. Cinquin, Y. Manioulouxand L. Cima, "Novel magnetic field and current sensors based on superparamagnetic transducers," *Sensor Letters*, Vol. 7, No. 3, 1–6, 2009.
7. Prokopovich, D. V., A. V. Popov, and A. V. Vinogradov, "Analytical and numerical aspects of bragg fiber design," *Progress In Electromagnetics Research B*, Vol. 6, 361–379, 2008.
8. Steinbauer, M., R. Kubasek, and K. Bartusek, "Numerical method of simulation of material influences in MR tomography," *Progress In Electromagnetics Research Letters*, Vol. 1, 205–210, 2008.
9. Ozgun, O. and M. Kuzuoglu, "Finite element analysis of electromagnetic scattering problems via iterative leap-field domain decomposition method," *Journal of Electromagnetic Waves and Applications*, Vol. 22, No. 2–3, 251–266, 2008.
10. Urbani, F., "Numerical analysis of periodic planar structures on uniaxial substrates for miniaturization purposes," *Progress In Electromagnetics Research Letters*, Vol. 5, 131–136, 2008.
11. Néel, L., "Influence des fluctuations thermiques sur l'aimantation de grains ferromagnetiques très fins," *Compte Rendu Hebdomadaire de Séance de l'Académie des Sciences*, Vol. 228, 664–666, 1949.
12. Néel, L., "Théorie du traînage magnétique des ferromagnétiques en grains fins avec application aux terres cuites," *Annales de Géophysique*, Vol. 5, 99–136, 1949.
13. Bean, C. P., "Hysteresis loops of mixtures of ferromagnetic micropowders," *J. Appl. Phys.*, Vol. 26, No. 11, 1381–1383, 1955.

14. Bean, C. P. and J. D. Livingston, "Superparamagnetism," *J. Appl. Phys.*, Vol. 30, 120S–129S, 1955.
15. Gleich, B. and J. Weizenecker, "Tomographic imaging using the nonlinear response of magnetic particles," *Nature*, Vol. 435, No. 7046, 1173-4, 2005.
16. Pankhurst, Q. A., J. Connolly, S. K. Jones, and J. Dobson, "Applications of magnetic nanoparticles in biomedicine," *J. Phys. D: Appl. Phys.*, Vol. 36, R167–R181, 2003.
17. Arruebo, M., R. Fernandez-Pachero, M. R. Ibarra, and J. Santamaria, "Magnetic nanoparticles for drug delivery," *Nanotoday*, Vol. 2, No. 3, 22–32, 2007.
18. Raj, K., R. Moskowitz, and R. Casciari, "Advances in ferrofluid in ferrofluid technology," *J. Magn. Magn. Mater.*, Vol. 149, 174–180, 1995.
19. Ravaud, R. and G. Lemarquand, "Design of ironless loudspeakers with ferrofluid seals: Analytical study based on the coulombian model," *Progress In Electromagnetics Research B*, Vol. 14, 285–309, 2009.
20. Kneller, E. and F. E. Fand Luborsky, "Particle size dependence of coercivity and remanence of Single domain particles," *J. Appl. Phys.*, Vol. 34, 656–658, 1963.
21. Cullity, B. D. and C. D. Graham, *Introduction to Magnetic Materials,* 2nd edition, Wiley-IEEE Press, 2008.